

# 1

## Hemodynamics and Hemorheology

Thomas PODGORSKI

CNRS, Université Grenoble Alpes, France

### 1.1. Structure and function of the circulatory system

Since the founding discovery by William Harvey, who demonstrated blood circulation in *De motu cordis* (Harvey and Leake 1928), blood and its circulation have received constant and renewed attention from doctors, physicists and fluid mechanics engineers. Further to Stephen Hales performing the first blood pressure measurements on horses (Hales 1733), Poiseuille (1835), motivated by a desire to understand blood flows at different scales, laid a solid foundation for rheology and fluid mechanics by establishing, through experimentation, the relationship linking flow rate, pressure drop and viscosity in a tube (Poiseuille 1844). More recently, these questions have formed the subject of numerous experimental, theoretical and numerical studies, in vivo and in vitro, with interest constantly renewed in light of technical and conceptual developments (imaging, velocimetry, rheometry, numerical methods, microfluidics, etc.) and ever greater coupling of different fundamental studies on model systems, clinical studies and questions of biomedical interest. The complexity of the cardiovascular system, which presents a multi-scale structure with time-dependent dynamics, regulated by numerous biological, physical and mechanical processes, cannot necessarily be reduced to the sum of its constituents or elementary behaviors, which interact in a nonlinear manner. Nevertheless, a quantitative understanding of this complexity always requires the study of

*Biological Flow in Large Vessels,*

coordinated by Valérie DEPLANO, José-Maria FULLANA, Claude VERDIER. © ISTE Ltd 2022.

simpler subsystems or configurations, in order to validate the physical concepts incorporated into larger scale models.

Blood circulation performs a number of essential physiological functions, including:

- transport of oxygen and nutrients from the lungs and digestive tract to tissues, and to or from storage organs and tissues (liver and adipose tissues);
- elimination of carbon dioxide and metabolic wastes to the lungs and disposal organs, thus participating in the regulation of the internal medium;
- immune response by transporting leukocytes and antibodies, and injury repair processes, notably via coagulation processes;
- transport of internal messengers (hormones) and medicines, ensuring their rapid distribution throughout the body.

The circulatory system is composed of a pump (the heart) and a complex network of vessels in which blood circulates, which can be divided into two parts: pulmonary circulation and systemic circulation. As pulmonary circulation takes place in a shorter circuit close to the heart, the pressure is lower there (from about 3.3 kPa or 25 mm Hg in the right ventricle and the pulmonary artery to 0.6 kPa, or 5 mm Hg in the left atrium) than in systemic circulation, where the distances to be covered and the amount of tissue to be irrigated are greater (from about 13 kPa [100 mm Hg] in the left ventricle and the aorta, to 0.6 kPa [5 mm Hg] in the right atrium). Vessel diameters extend across almost five orders of magnitude, from the largest arteries (several cm) to the finest capillaries (several  $\mu\text{m}$ ), with average velocities ranging from about 1 mm/s in capillaries to almost 1 m/s in the aorta, with a highly pulsed flow linked to the heart's operation in the arteries and veins close to the heart: during systole (contraction of the heart), the pressure reaches approximately 120 mm Hg (16 kPa) in the aorta and 25 mm Hg (3.3 kPa) in the pulmonary artery, and drops sharply within the heart during diastole. This results in very different natures of flow depending on the position in the network. These flows can be characterized by two dimensionless numbers: the Reynolds number,  $Re = \rho UD/\eta$ , where  $\rho$  is the blood density (about 1,060 kg/m<sup>3</sup>),  $U$  is the typical flow velocity,  $D$  is the vessel diameter and  $\eta$  is the dynamic viscosity (about 3–4 mPa·s); and the Womersley number,  $\alpha = R(\omega\rho/\eta)^{1/2}$ , where  $R$  is the vessel radius and  $\omega$  is the pulsation (of the order of 20 rad/s for a heart rate of 60 beats/min). The typical values of these numbers in the different stages of circulation are given in Table 1.1. These values show that, first, flows are highly inertial in

the large vessels (arteries and veins) for which  $Re \gg 1$ , whereas in the finer vessels they are dominated by viscous effects and, second, the effects of the pulsed nature of the flow are mainly felt in the large vessels where  $\alpha > 10$ . The consequence of these large values of the Womersley number is that the velocity profile in these vessels does not have time to develop completely and is relatively flat, and that Poiseuille's law, for example, does not apply. In finer vessels, the viscous effects, combined with the elasticity of the upstream vascular walls, enable dampening of the pressure fluctuations and flow there is quasi-stationary. Wall shear rate, a significant parameter for the function of the endothelium lining the vessels, also varies significantly, with a maximum in the arterioles.

	Diameter (mm)	Average velocity (mm/s)	Reynolds, $Re$	Womersley $\alpha$	Wall shear rate (1/s)
Aorta	25	400	3,000	17	130
Arteries	4	450	550	3	900
Arteriole	0.05	50	0.75	0.03	8,000
Capillary	0.008	1	0.002	0.006	1,000
Venule	0.02	2	0.01	0.01	800
Veins	5	100	150	3	160
Vena cava	30	380	3,500	20	100

**Table 1.1.** Typical values of flow parameters in different levels of the vascular network

Besides their geometric properties, the structure and mechanical properties of vessels contribute to circulatory dynamics through passive dilatation/relaxation mechanisms and active contraction/expansion mechanisms. Vascular walls are multi-layer structures presenting variations depending on their position in the vascular network, and therefore different mechanical properties. The internal surface of the vessels, common to the entire vascular system, consists of a layer of endothelial cells whose elongated shape varies with local shear stresses. The endothelium fulfills several exchange functions between blood, the vascular wall and surrounding tissues. It intervenes in the immune response through the processes of adhesion and extravasation of circulating cells, and also regulates coagulation and vasomotor processes and intervenes in angiogenesis. Endothelial cells are sensitive to hydrodynamic and mechanical stresses, thus allowing short-term adaptation

(vasoconstriction/vasodilatation) or longer term remodeling and adaptation via growth, migration or apoptosis of vascular cells. The presence of this nucleated cell layer on the inner surface of the vessels results in surface roughness, with height variations of up to 750 nm in endothelial cell nuclei. The shape of the cells, 10–15  $\mu\text{m}$  wide and 60–100  $\mu\text{m}$  long in the flow direction, adapts to local stresses. In addition, the surface of these cells is covered with a layer of glycoproteins and glycolipids forming a brush (glycocalyx), which plays a crucial role in hemostasis and coagulation, or the regulation of vasomotor processes (Reitsma *et al.* 2007; Weinbaum *et al.* 2007).

The walls of the large vessels have a layered, *tunic*-shaped structure successively composed, from the inside to the outside, of (i) the *intima*, composed of the endothelium and the underlying connective tissue, the internal elastic lamina whose thickness, structure and properties depend on the vessel type, (ii) the *tunica media*, composed of circumferential, smooth muscle cells, collagen and elastic tissue, and (iii) the *tunica externa* (*adventitia*), composed mainly of connective tissue (collagen and elastin), but also, for the large nerve arteries, of small vessels irrigating the arterial wall (*vasa vasorum*) and lymphatic vessels.

A common pathology of the arterial wall is atherosclerosis, which leads to coronary heart disease due to the progressive formation of atheromatous plaque in the artery, resulting in a narrowing of the lumen. It results from chronic inflammation of the arterial wall, which is most likely to occur in zones of disturbed flow, such as branches. It generally begins with endothelial dysfunction and disruptions in the elastin layer, causing the subendothelial accumulation of cholesterol (LDL), which forms atheroma by mixing with cell debris and becoming surrounded by a fibrous shell (Weber and Noels 2011).

Veins, which have thinner walls (thin *intima*, quasi-absent internal elastic lamina and weak *media* except in the lower limbs) and a more elliptical than circular cross-section, generally behave more passively than arteries. Medium-caliber veins generally feature valves with folding *intima*, which prevent backflow.

The small vessels have a simpler structure, composed of an endothelium surrounded by one or more layers of smooth muscle cells for the arterioles, allowing flow to be regulated in the organ concerned. The capillaries consist

of an endothelium supported by a basal membrane, whose structure and permeability depend on the organ (continuous and slightly permeable membrane in the muscles, lungs and skin, discontinuous and highly permeable in the glands, mucous membranes, liver, spleen, bone marrow, etc.). The postcapillary venules have a structure close to the latter, while the largest venules have smooth muscle cells.

The conditions and nature of flows are strongly influenced by the size, geometry and mechanical properties of the vascular walls. In the largest vessels, flows are inertial (generally without turbulence), often unsteady and may present secondary flows such as recirculations. In small vessels with a diameter less than a few dozen times the size of blood cells, the multiphase nature of the blood can no longer be reduced to a continuous medium-type approach, and a specific rheology is manifested. The following sections summarize the structure and rheological properties of blood in these different situations.

## 1.2. Blood composition

Blood is a complex fluid in terms of its composition and rheology. It is a dense suspension of generally deformable objects (blood cells) in a fluid with a composition that can be complex to a lesser or greater degree, plasma. A simple centrifugation of a whole tube of blood essentially reveals three fractions which, in order of increasing density, are a fluid phase containing various solutes (plasma), a layer called the buffy coat, consisting of leukocytes (white blood cells) and platelets representing less than 1% of the total volume, and a dense layer of red blood cells (erythrocytes or red corpuscles) representing a volume fraction (hematocrit) of 38–46% in women and 42–53% in men, or about 45% on average. The different blood cell types are summarized in Table 1.2.

Plasma is composed mainly of water (92%), proteins (7%), electrolytes (0.9%), lipoproteins and lipids (0.6%) and carbohydrates (0.1%). Electrolytes (predominantly  $\text{Na}^+$ , followed by  $\text{Ca}^{++}$ ,  $\text{K}^+$ , and  $\text{Mg}^{++}$  for cations and predominantly  $\text{Cl}^-$ , followed by  $\text{HCO}_3^-$ ,  $\text{HPO}_4^{2-}$  and  $\text{So}_4^{2-}$  for anions) control osmotic pressure, are regulated by the kidneys and are involved in cellular processes. Carbohydrates are energy sources for cells, and are divided into oligosaccharides (glucose, fructose and galactose), disaccharides (sucrose, lactose and maltose) and polysaccharides (glycogen). Lipoproteins are structures that encapsulate insoluble lipids (cholesterol and

triglycerides) in a shell of polar lipids and proteins. They are divided into chylomicrons, very low-density lipoproteins (VLDL), low-density lipoproteins (LDLs) and high-density lipoproteins (HDLs), which differ in size and content (80–500 nm for chylomicrons to 10 nm for HDLs) and participate in different functions.

Proteins, a number of which play a crucial role in blood rheology, are divided into different families representing different plasma fractions. Fibrinogen (0.03% or 195–365 mg/dL) acts on red blood cell aggregation (see section 1.5.2) and is involved in coagulation. Albumin is the main plasma protein (0.6% or 3.3–4.5 g/dL), used for the transport of small molecules and at this concentration level has a significant contribution to plasma osmolarity. Globulins ( $\alpha$ ,  $\beta$ ,  $\gamma$ -globulins) and antibodies represent about 0.4% of plasma in total. Finally, other nitrogenous compounds are present, such as urea, ammonium salts, uric acid, creatine, creatinine and amino acids, many of which are waste eliminated by the kidneys.

Cell type	Count / $\mu$ L	Geometry
Red blood cells (erythrocytes), ~99.7%	~5,000,000	Biconcave disc diameter 8 $\mu$ m, thickness 2.5 $\mu$ m
White blood cells (leukocytes), ~0.2%	~7,500	Quasi-spherical diameter 20–100 $\mu$ m
Platelets (thrombocytes), ~0.1%	~250,000	Ellipsoid major axis 4 $\mu$ m, minor axis 1.5 $\mu$ m

**Table 1.2.** Blood cell types, relative fraction and geometrical data

In rheological and modeling terms, plasma is generally considered as a Newtonian fluid with a viscosity between 1.1 and 1.3 mPa·s (normal values independent of age and gender). However, recent studies involving a complete rheological characterization and molecular simulations of protein dynamics at high shear and extension rates have shown that it is viscoelastic in nature at high frequencies (Varchanis *et al.* 2018). Although the deformation rates considered ( $10^3$  to  $10^5$  s<sup>-1</sup>) are higher than those encountered in most of the vascular network (Table 1.1), these non-Newtonian effects could be significant in regions such as the arterioles or capillaries.

Among the factors that have a crucial influence on blood rheology, hematocrit plays a leading role, with an indirect influence on the mechanical

properties of red blood cells (see section 1.3). As in any suspension, the effective viscosity and possible viscoelastic properties increase with the volume fraction in particles. The hematocrit varies significantly around the mean value of 45%, with, first, a significant difference between men and women under normal conditions and, second, pathological deviations toward lower values (anemia) or higher values (polycythemia), resulting in significantly different blood viscosities, and thus an altered oxygen transport capacity. There are different types of anemia, which may be due to a hemorrhage, the destruction of red blood cells by different pathologies (see section 1.3) or a deficit in hemoglobin production. Polycythemia may result from adaptation to conditions of reduced oxygenation (living at high altitude, sleep apnea syndrome, etc.) or from diseases such as polycythemia vera (Vaquez disease), a myeloproliferative syndrome that can double, or more than double, the number of red blood cells (these are then often smaller than normal) and bring the hematocrit to above 55%. Finally, certain doping techniques in sport essentially aim to increase hematocrit to improve blood oxygenation capacity – with the circulatory risks that doing so entails – thus enabling blood viscosity to be doubled, with a 40–60% increase in hematocrit. It should be noted that even in the absence of doping or pathological conditions, hematocrit and blood viscosity may vary significantly during physical exercise due to dehydration or fluid exchange with the rest of the body, which may modify the ratio of red blood cell and plasma volumes (Connes *et al.* 2013). Strictly from the point of view of oxygen transport efficiency, there is an optimal concentration for blood systems (Jensen *et al.* 2013), ensuring maximum transport, otherwise equal in all aspects (with imposed pressure or pumping power): the transported flow is proportional to the concentration (hematocrit), but an increase in this concentration is accompanied by an increase in viscosity, such that between two extremes (zero hematocrit, for which the red blood cell flow is zero by definition, and maximum hematocrit, for which the viscosity is such that the flow stops), an optimum exists, located more or less in the physiological hematocrit range. This optimum may be influenced by a number of factors, such as the properties of red blood cells, but also other blood or extra-blood factors (Reinhart 2016). It should be noted, for example, that the mean hematocrit value varies significantly between different animal species (mammals, birds, reptiles and amphibians), with normal values ranging from 20% to 55% for highly variable red blood cell volumes, shapes and deformabilities (Hawkey 1975; Lewis 1996). The following section summarizes the properties of the human red blood cell, its pathologies and its dynamics.

### 1.3. The red blood cell: structure and dynamics

#### 1.3.1. *Red blood cell properties*

The primary function of red blood cells is to transport oxygen and eliminate carbon dioxide from the body. The main oxygen carrier is hemoglobin, an organometallic protein contained in the cytoplasm of red blood cells, which has the ability to fix an amount of oxygen that is much higher than the solubility limit of plasma. The extraction of  $\text{CO}_2$  is assisted by carbonic anhydrase, an enzyme located in the red blood cell membrane catalyzing the hydration of carbon dioxide into  $\text{H}_2\text{CO}_3$ , which dissociates into  $\text{HCO}_3^-$  bicarbonate ions and  $\text{H}^+$  protons, thus having an effect on blood pH, combined with the role of hemoglobin as a buffer.

Red blood cells, which lack nuclei, have a characteristic biconcave disc shape with an average diameter of  $7.7 \pm 0.7 \mu\text{m}$  and a thickness at the thickest point of about  $2.8 \pm 0.5 \mu\text{m}$  and about  $1.4 \pm 0.5 \mu\text{m}$  in the center (Evans and Fung 1972). The mean corpuscular volume (MCV), which is an essential hematological parameter, is on average between  $82$  and  $98 \mu\text{m}^3$ , while the membrane surface area is about  $140 \mu\text{m}^2$ . These characteristics make it a highly deflated object (the red blood cell's membrane surface could contain a volume of about  $150 \mu\text{m}^3$  if it were spherical in shape) that allows for substantial deformations, notably in order to circulate within the finer capillaries, whose diameter is less than  $8 \mu\text{m}$ . In theoretical models that require the characteristics of the model object representing the red blood cell to be fixed, a dimensionless parameter is generally defined. This may be a reduced volume (corpuscular volume/volume of a sphere with the same surface area), having a value of about 0.59 for an average blood cell, or a relative excess surface area (membrane surface/surface of a sphere of the same volume) of about 1.44 on average.

Since the cell is devoid of a nucleus and organelles, its internal medium essentially consists of a solution of hemoglobin (cytosol), which is considered as a Newtonian fluid (the range of shear rates accessible in this compartmentalized medium being restricted). The mean concentration of hemoglobin in cytosol (mean corpuscular hemoglobin concentration in hematology) is normally comprised between 32 and 36 g/dL. This concentration is responsible for the relatively high value of the internal viscosity of red blood cells. Since this concentration range is just below the solubility limit of hemoglobin, the viscosity can vary significantly, from 6 mPa·s at 32 g/dL to 10 mPa·s at 36 g/dL at 37°C (Ross and Minton 1977).

However, this mean value masks a significant dispersion within the same blood sample. Indeed, red blood cells that are produced in bone marrow from hematopoietic stem cells before being released into the circulation have an average lifespan of 120 days. Over this duration, their density increases due to dehydration (approximately 1,060 to 1,120 g/L), resulting in a 25–30% increase in the corpuscular hemoglobin concentration. The concentration within the individual red blood cells of the same sample can thus range from 19 to 25 mmol/L or 30–40 g/dL (Bosch *et al.* 1992), and corresponding viscosity variations from 5 to 20 mPa·s. This significant increase in red blood cell viscosity, combined with membrane alterations, significantly reduces their deformability (Linderkamp *et al.* 1993) and leads to their elimination by the spleen through a process of filtration and phagocytosis. The viscosity of hemoglobin is also sensitive to other parameters such as temperature and calcium concentration, and presents a transition within the vicinity of body temperature, notably for high hemoglobin concentrations (Kelemen *et al.* 2001). The internal viscosity of red blood cells is thus significantly higher at room temperature (20–25°C) than at 37°C, which may be a factor to be taken into consideration in the interpretation of *in vitro* experiments whose temperature is not necessarily regulated. Furthermore, the dispersion of hemoglobin concentration and viscosity values within the same sample and the influence that this dispersion may have on the red blood cell dynamics in flow represents a challenge for modeling and numerical simulations focusing on collective behavior.

The membrane consists of a phospholipid bilayer containing inclusions of transmembrane proteins (Band-3 ion channels, glycoporphins carrying antigens of the blood group, notably). Below the inner surface of the membrane is a cytoskeleton consisting of a dense network of spectrin filaments bound to the membrane by complexes involving anchoring proteins (association of spectrin-ankyrin-protein 4.2-band 3, or spectrin-actin-protein p55-protein 4.1-glycophorin C). These interactions allow the structural integrity of the red blood cell to be maintained. The phospholipid bilayer, which is a two-dimensional fluid, confers several significant mechanical properties to the red blood cells. The most obvious is a quasi-inextensibility with a surface expansion module (ratio between isotropic surface tension and relative surface expansion) of about 400 mN/m, an important value at the scale of a micrometer object. In practice, the surface area of the membrane can therefore be considered constant, with dilatations not exceeding 5% for hydrodynamic stresses, such as those experienced in circulation. The membrane also has a bending resistance that

is generally modeled by a Canham–Helfrich energy per unit surface taking the following form (Helfrich 1973; Seguin and Fried 2014):

$$E_b = \frac{1}{2} \kappa (H - H_0)^2 + \kappa_G G \quad [1.1]$$

where  $\kappa$  is the curvature modulus with a value of  $1.15 \pm 0.9 \times 10^{-19}$  J,  $H$  is the local mean curvature,  $H_0$  is the spontaneous curvature (linked to the asymmetry of the two lipid layers),  $\kappa_G$  is the Gaussian curvature modulus and  $G$  is the Gaussian curvature. With  $G$  being a topological invariant, the second term is therefore constant and only the first term is likely to vary with deformations of the membrane. It is essentially this bending elasticity that is responsible for the biconcave equilibrium shape of the red blood cell, which minimizes the integral of the bending energy at a given surface area and volume. Finally, friction between phospholipids and with transmembrane proteins produces a surface viscosity that plays a non-negligible role in the dynamics of the red blood cell.

In parallel with the fluid membrane, the spectrin network is an elastic shell characterized by a shear modulus of approximately  $5 \mu\text{N/m}$  (Table 1.3). The question of the reference shape of this elastic component (a shape for which the stresses are zero) remains a matter of debate (Švelc and Svetina 2012). Several hypotheses have been put forward, with some taking into account the formation of the red blood cell, and different shapes have been proposed, from a spherical reference shape (which assumes that the cytoskeleton retains a memory of its composition in an initially quasi-spherical cell with a nucleus) to a biconcave reference shape (which assumes that slow remodeling of the cytoskeleton leads it to relax toward the shape imposed by the minimization of the membrane bending energy). This question is far from anecdotal in the modeling of quantitative red blood cells, and numerical simulations have shown the influence of this choice in different situations (Hoore *et al.* 2018).

Since previous results showed a link between red blood cell metabolic activity and deformability (Weed *et al.* 1969), several works have suggested possibilities for remodeling the spectrin network and its links with the membrane involving ATP (adenosine triphosphate), which could provide the energy needed for this remodeling, and thus modulate the shape and deformability of the red blood cell to optimize its function in the microcirculation (Park *et al.* 2010). Other works also suggest that the high

stresses experienced by the red blood cell in the microcirculation lead to the release of ATP in the plasma, which could in turn serve as a signal to endothelial cells to trigger vasomotion mechanisms and adapt the resistance of the microcirculation network (see WAN *et al.* (2011) for a review). However, these possible interactions between ATP, red blood cell mechanical properties and signaling still remain to be fully clarified and are even a contentious issue (Betz *et al.* 2009).

The mean values of the main mechanical properties of the healthy red blood cell are summarized in Table 1.3. A review of the techniques for measuring these different properties is given in Tomaiuolo (2014).

	Mean values
Volume ( $\mu\text{m}^3$ )	$89.4 \pm 17.6$
Surface area ( $\mu\text{m}^2$ )	$138.1 \pm 27.6$
Internal viscosity ( $\text{mPa}\cdot\text{s}$ )	$6.07 \pm 3.8$
Membrane viscosity ( $\mu\text{N}\cdot\text{s}/\text{m}$ )	$0.7 \pm 0.2$
Membrane shear modulus ( $\mu\text{N}/\text{m}$ )	$5.5 \pm 3.3$
Bending energy ( $\times 10^{-19}$ J)	$1.15 \pm 0.9$
Surface compressibility modulus ( $\text{mN}/\text{m}$ )	$399 \pm 110$

**Table 1.3.** Main red blood cell mechanical parameters and typical values (according to Tomaiuolo (2014))

### 1.3.2. Erythrocyte pathologies

A number of conditions of congenital, infectious or metabolic origin are likely to significantly alter the properties of the red blood cell, and consequently the rheology of the blood. With regard to the mechanical and modeling consequences, they can affect the properties of the cytosol or the membrane, together with morphological modifications.

There are several hereditary hemoglobinopathies, the most emblematic of which is drepanocytosis (sickle cell disease), which affects around 300,000 births a year worldwide (Rees *et al.* 2010). It is caused by a mutation in a hemoglobin gene that results in the production of an abnormal hemoglobin, hemoglobin S (HbS). In homozygous patients, the high HbS concentration in red blood cells leads to its polymerization under low oxygen pressure conditions (notably when red blood cells deoxygenate substantially in the

microcirculation in situations of effort, stress and dehydration). This results in a rigidification of the red blood cells and, depending on the rate at which deoxygenation has occurred, a change in shape related to the polymerization of HbS in the form of fibers. The red blood cells then take on the characteristic shape of a rigid sickle, which can cause capillary occlusions (Figure 1.1). Altered red blood cells are also more fragile, resulting in hemolytic anemia (Figure 1.2). The severe complications, high prevalence of the disease, and the difficulty of its treatment make it an important topic of study for therapeutic purposes and diagnostic aid. Blood rheology is altered by several factors interacting in a complex manner (hematocrit, and composition of the plasma, which is generally more viscous due to increased protein concentration) and more widely speaking, an increase in viscosity is observed, even in oxygenated blood, due to a reduced deformability of the red blood cells (Barabino *et al.* 2010).

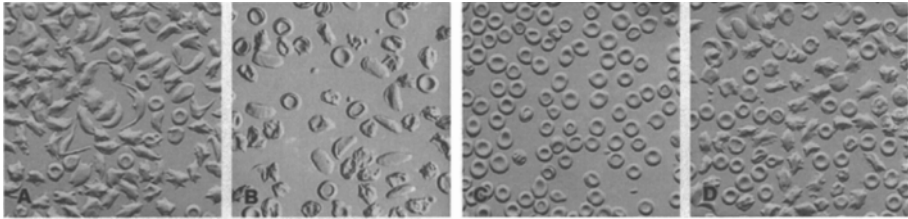


**Figure 1.1.** Sickle-cell morphologies under different oxygen partial pressures: (a–c) venous (deoxygenated) blood from three different patients; (d) after oxygenation of sample B with 25%  $O_2$  ( $PO_2 = 180$  mm Hg) (Asakura *et al.* 1994). Copyright National Academy of Sciences, U.S.A (1994)

A hemoglobinopathy commonly associated with sickle cell disease is hemoglobinosis C, caused by the production of another type of abnormal hemoglobin, HbC. This abnormal hemoglobin is less likely to polymerize than HbS, but still leads to a decrease in red blood cell deformability. In addition, the prevalence of HbC and HbS genes in the same populations means that HbSC heterozygotes are more common than HbCCs (Nagel *et al.* 2003).

Thalassemias ( $\alpha$  or  $\beta$  depending on the type of hemoglobin subunit affected) are another family of highly prevalent hereditary hemoglobinopathies (Higgs *et al.* 2012). They are characterized by hypochromia (hemoglobin deficiency and therefore a lower internal viscosity) and microcytosis (smaller than normal red blood cells).

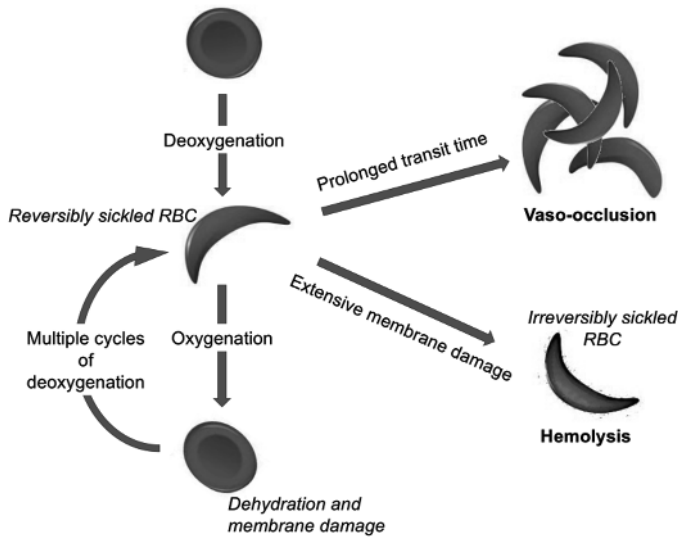


**Figure 1.2.** Sickling, hemolysis and capillary occlusion in sickle cell disease (according to Kumar et al. (2012)). For a color version of this figure, see [www.iste.co.uk/deplano/biological.zip](http://www.iste.co.uk/deplano/biological.zip)

Red blood cells maintain their biconcave shape (favoring their deformability) by regulating osmotic exchanges through their membrane. In particular, the internal sodium and calcium concentrations are maintained at a low level because of the ion channel activity (requiring energy in the form of ATP to function). A genetic modification of the AE1 anion exchanger (band 3) making it permeable to cations is linked to several forms of stomatocytosis, the most common form of which leads to dehydration of the red blood cells, and thus both an increase in internal viscosity and a change in shape (Da Costa *et al.* 2013). A number of hereditary membrane pathologies affect the cytoskeleton and lead to changes in the geometry of the red blood cell: spherocytosis, elliptocytosis, ovalocytosis, etc. The defects, which affect either the links between the cytoskeleton and the membrane, or the interactions within the spectrin network, lead to fragility of the membrane and a loss of its surface area to a lesser or greater degree, leading to an alteration in the shape and deformability of the red blood cells. Figure 1.3 shows several examples of morphological alterations associated with these pathologies, as well as the mechanical consequences characterized by the measurement of an elongation index in ektacytometry.

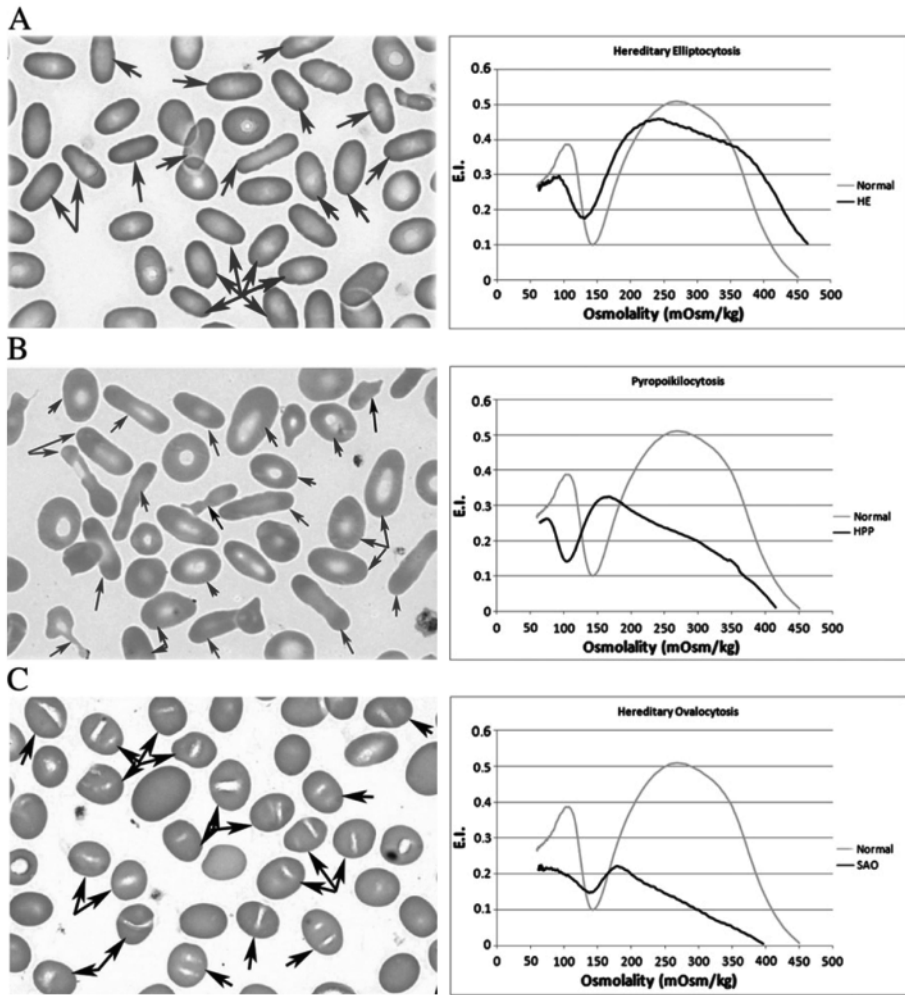


**Figure 1.3.** Examples of red blood cell membrane pathologies. a) Elliptocytosis, b) pyropoikilocytosis and c) ovalocytosis. The graphs represent measurements of deformability by ektacytometry (elongation index, E.I.) as a function of the osmolality of the medium. The light-colored curve represents normal red blood cells (according to Da Costa et al. (2013)). For a color version of this figure, see [www.iste.co.uk/deplano/biological.zip](http://www.iste.co.uk/deplano/biological.zip)

### 1.3.3. Red blood cell dynamics

As we saw above, a number of questions remain open regarding the structure and mechanical properties of the red blood cell, notably regarding the values and variability of membrane properties: bending rigidity, elastic modulus and membrane viscosity. The question of the reference shape of the cytoskeleton is also significant and unresolved: is this shape fixed, if so which shape is it, or is it subject to remodeling? Should these properties be considered fixed, or dynamic and capable of adapting to the flow through ATP-consuming active mechanisms? The alteration of the mechanical properties of red blood cells can be a consequence (and an indicator) of different hemoglobin and membrane pathologies, with repercussions on blood rheology: the dynamics of red blood cells (deformations, orientation with respect to flow) depend directly on them and condition the viscous dissipation, the elasticity of the suspension and the hydrodynamic interactions responsible for structuring under flow.

A simple shear flow is a reference rheometric configuration, in which the dynamics of a suspended red blood cell can be considered as a marker of its rheological properties. It is also a useful reference configuration to contrast theoretical and numerical models and compare them with the experiment, in order to validate their usage in more complex flows.

Many theoretical approaches have been proposed for modeling red blood cells, including models of elastic capsules (see, for example, Lac and Barthès-Biesel (2005)) or vesicles (Vlahovska *et al.* 2009; Biben *et al.* 2011). While these models, in their simple version (two-dimensional, incompressible fluid with bending elasticity for vesicles, quasi-two-dimensional solid with dilatation and shear elasticity for capsules), enable a number of red blood cell behaviors to be described in qualitative terms, more recent models tend to incorporate, to as great a degree as possible, the set of mechanical parameters that can influence the dynamics (inextensibility, bending and shear elasticity, and membrane viscosity). Many recent works focus on simple-shear red blood cell dynamics (see, in particular, Cordasco and Bagchi (2014), Peng *et al.* (2014), Sinha and Graham (2015), Lanotte *et al.* (2016) and Mauer *et al.* (2018)). On the experimentation side, a number of recent studies have confirmed or identified different dynamic regimes (Dupire *et al.* 2012; Fischer and Korzeniewski 2013; Lanotte *et al.* 2016; Levant and Steinberg 2016; Mauer *et al.* 2018) for the purpose of drawing up a diagram of the transitions between different motions of tank

treading, tumbling, rolling and other more complex motions combining rotations, oscillations or deformations.

The parameters influencing dynamics (viscosities of internal ( $\eta_i$ ) and external ( $\eta_o$ ) fluids, membrane viscosity, bending ( $\kappa$ ) and shear ( $\mu$ ) moduli, flow shear rate  $\dot{\gamma}$ , volume ( $V$ ) and surface area ( $S$ ) of the blood cell) are generally combined into a set of dimensionless numbers that are the reduced volume ( $\nu$ ), viscosity ratio ( $\lambda$ ) and capillary numbers ( $Ca_\kappa$  and  $Ca_\mu$ ) comparing the viscous stresses with the forces linked to the bending or shear elasticity of the membrane. These parameters are defined by:

$$\begin{aligned}\lambda &= \eta_i / \eta_o \\ \nu &= \frac{V}{\frac{4}{3}\pi\left(\frac{S}{4\pi}\right)^{\frac{3}{2}}} \\ Ca_\kappa &= \frac{\eta\dot{\gamma}\left(\frac{3V}{4\pi}\right)}{\kappa} \\ Ca_\mu &= \frac{\eta\dot{\gamma}\left(\frac{3V}{4\pi}\right)^{\frac{1}{3}}}{\mu}\end{aligned}\tag{1.2}$$

where  $(3V/4\pi)^{1/3}$  is the mean radius of the red blood cell, defined as the radius of a sphere of the same volume.

Despite many dynamic modes having been identified in different studies, and the fact that the transitions between different regimes can be hysteretic in nature (Dupire *et al.* 2012), there is still no consensus regarding the general diagram of the shear red blood cell dynamics to serve as a common reference for validating theoretical and numerical models. It should be noted that variability in the properties of red blood cells between different subjects and within a sample from a given subject may be a cause of the differences observed between different experimental studies. To account for this property dispersity, a recent study statistically quantified cell populations in the different dynamic modes by measuring the orientations and shapes of a large number of cells within the same shear sample (Minetti *et al.* 2019). By

confirming the variety of dynamic modes, the ranges of parameters on which transitions occur and quantifying the fractions of the red blood cell population in the different modes, these statistical data complete the landscape of a reference flow situation for modeling (Figure 1.4).

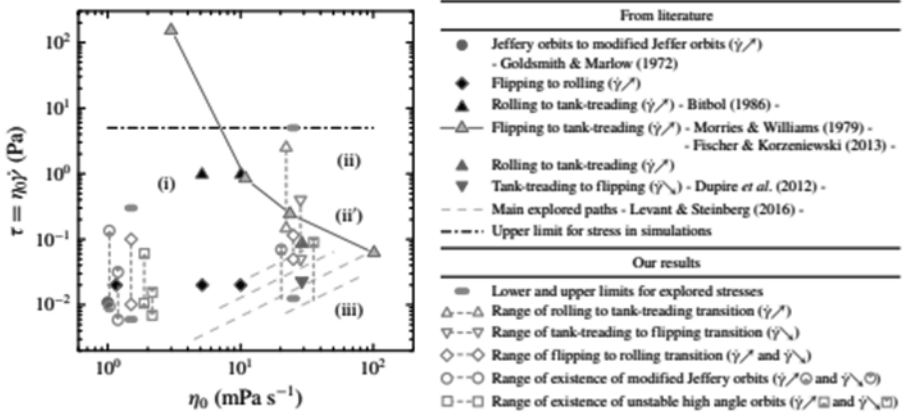


**Figure 1.4.** Transitions between dynamic regimes of the shear red blood cell identified in the literature and transition ranges observed on a large sample of red blood cells (Minetti *et al.* 2019). For a color version of this figure, see [www.iste.co.uk/deplano/biological.zip](http://www.iste.co.uk/deplano/biological.zip)

## 1.4. Rheology and dynamics

### 1.4.1. Phenomenology of blood rheology

From a macroscopic point of view, that is to say, at measurement scales significantly higher than that of the cellular constituents, the behavior presented by blood for shear rates typical of those encountered in large vessels ( $10^2$ – $10^3$   $s^{-1}$ ) is quasi-Newtonian, with a viscosity of the order of 3–4  $mPa \cdot s$ . This simple rheology can be useful for modeling flows in large vessels in their broad outline (Ku 1997), in particular through the use of solvers of the Navier–Stokes equations in numerical simulation. Notably, it has been shown that at the scale of the large arteries, the imaging resolution does not make it possible to systematically distinguish significant non-Newtonian effects, and that a Newtonian rheology is sufficient in order to reasonably describe the flows as a whole – that is, in terms of pressure distributions and flow rates – in arteries that can measure as little as 5 mm in diameter, with renormalization of the viscosity (Lee and Steinman 2007).

This simplified perspective, nevertheless, masks a complexity that may be significant in specific regions of physiological flows or in artificial systems, and when considering details that can be crucial in pathological situations, and situations of biomedical interest, or in intermediate regions of the vascular tree. In these situations, it may be necessary to take into account the non-Newtonian aspects of blood rheology.

An essential phenomenon of constant-shear rheology of blood is its shear-thinning nature (Chien 1970): in a range of shear rates from  $10^{-2}$  to  $10 \text{ s}^{-1}$ , blood viscosity falls by nearly two orders of magnitude, in direct relation to (i) the decrease in red blood cell aggregation and (ii) the influence of red blood cell deformability (Figure 1.5), the latter leading to a morphology and dynamics that depend on the shear rate. Several authors have focused on determining a blood yield stress resulting from the formation of aggregate networks at very low shear rates. These measurements at vanishing shear rates are technically difficult, notably due to artifacts related to red blood cell sedimentation, but it has been possible to produce estimates using a Casson law for rheology, in which the relationship between stress ( $\tau$ ) and shear rate  $\dot{\gamma}$  is given by:

$$\sqrt{\tau} = \sqrt{\tau_y} + \sqrt{\eta\dot{\gamma}} \quad [1.3]$$

where  $\tau_y$  is the yield stress. An adjustment of this type of law to rheometric measurements at low shear rates allows this yield stress to be estimated at about 5 mPa, under average physiological conditions (Picart *et al.* 1998).

On the circulatory side, shear-thinning, in particular associated with aggregation phenomena, can play a role at different levels. First, it can modify the velocity profiles by making them non-parabolic. In addition, for geometric reasons, secondary flow zones may appear transiently in the branches or curved portions of large vessels, constrictions (or irregularities related to the presence of stents, atherosclerosis etc.) due to the inertial, unsteady nature of the flow. A number of phenomenological rheological models are conventionally used in numerical simulation, from simple models such as power law or Carreau (Cho and Kensey 1991), to more elaborate models such as Carreau-Yasuda (Bird *et al.* 1987), modified Casson (Fung 1993), generalized power law (Ballyk *et al.* 1994) or Quemada (Quemada 1978). The latter model allows a good representation of blood rheology in steady shear to be obtained, avoiding the singular nature of the simple Casson model at near-zero shear rates, and the instabilities linked to the evolution of

aggregate structures to be taken into account. Furthermore, the Quemada model is equivalent to a modified Casson model (Buchanan *et al.* 2000). The generic forms of these different models are summarized in Table 1.4.

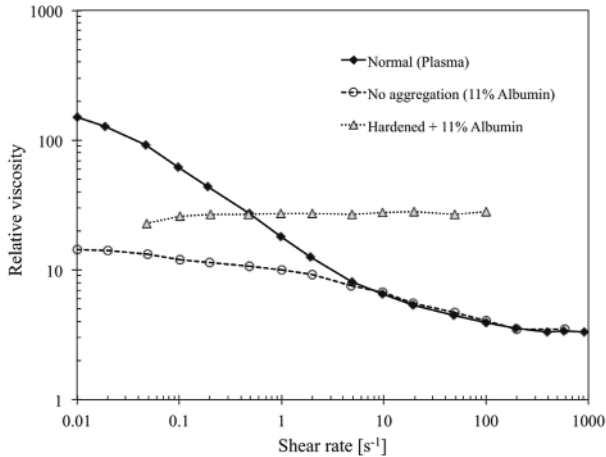


**Figure 1.5.** Relative viscosity (normalized by plasma viscosity) for a suspension of normal human red blood cells with a hematocrit of 45% in plasma (normal blood) in a buffer containing albumin (with no aggregation) and glutaraldehyde-stiffened red blood cells (data from Chien (1970))

The unsteady nature of blood flows in part of the vascular system, as well as the complex and variable cross-section flow geometries, lead us to consider the dynamic aspects of blood rheology. The characteristic times for the establishment of a microstructure related to red blood cell aggregation (as well as possible hysteresis in the force/distance relationship between the aggregation and disintegration processes; see section 1.5.2) are responsible for the thixotropic nature of blood. This has been revealed by a number of experimental measurements (Dintenfass 1962), but remains a weak and visible effect, mainly at low shear rates with relatively long relaxation times, and this effect is likely negligible under physiological flow conditions. Viscoelastic properties have been shown to emerge in frequency (or characteristic time) ranges relevant to blood circulation (Thurston 1973). Since these properties are closely related to the composition of blood and the mechanical properties of its constituents (red blood cell deformability), a quantitative understanding of the link between microscopic properties and viscoelastic characteristics may be of significant interest, in order to use rheology for diagnostic purposes, for example. However, this viscoelasticity

decreases significantly as the shear rate increases and for physiological hematocrits (McMillan *et al.* 1986), suggesting that in a vessel flow modeling approach, the main non-Newtonian characteristic to be taken into account remains the shear-thinning behavior.

Designation	Viscosity law	References
Power law	$\eta = k  \dot{\gamma} ^{n-1}$	(Cho and Kensey 1991)
Carreau	$\eta = \eta_{\infty} + (\eta_0 - \eta_{\infty})(1 + A  \dot{\gamma} ^2)^n$	(Cho and Kensey 1991)
Carreau-Yasuda	$\eta = \eta_{\infty} + \frac{\eta_0 - \eta_{\infty}}{(1 + \lambda  \dot{\gamma} ^b)^a}$	(Bird <i>et al.</i> 1987)
Modified Casson	$\eta = \left[ \sqrt{\tau_y \left( \frac{1 - e^{-m \dot{\gamma} }}{ \dot{\gamma} } \right)} + \sqrt{\eta_c} \right]^2$	(Fung 1993)
Generalized power law	$n = k(\dot{\gamma})  \dot{\gamma} ^{n(\dot{\gamma})-1}$ $k(\dot{\gamma}) = \eta_{\infty} + \Delta \eta \exp \left[ - \left( 1 + \frac{ \dot{\gamma} }{a} \right) \exp \left( \frac{-b}{\dot{\gamma}} \right) \right]$ $n(\dot{\gamma}) = n_{\infty} + \Delta n \exp \left[ - \left( 1 + \frac{ \dot{\gamma} }{c} \right) \exp \left( \frac{-d}{\dot{\gamma}} \right) \right]$	(Ballyk <i>et al.</i> 1994)
Quemada	$\eta = \frac{\eta_0}{\left[ 1 - \frac{1}{2} \left( \frac{k_0 + k_{\infty} \dot{\gamma}^{1/2}}{1 + \dot{\gamma}^{1/2}} \right) H \right]^2}$ <p>Equivalent shape (modified Casson):</p> $\eta = \left( \sqrt{\eta_{\infty}} + \frac{\sqrt{\tau_0}}{\sqrt{\lambda} + \sqrt{\dot{\gamma}}} \right)^2$	(Quemada 1978, Buchanan <i>et al.</i> 2000)

**Table 1.4.** Main models of macroscopic blood rheology

Taking this shear-thinning behavior into consideration, although it significantly complicates numerical simulations, leads to significantly different results from the Newtonian model in situations of medical interest in the presence of pulsatile flow, bifurcations or stenosis-like constrictions (Buchanan *et al.* 2000). As an example, Karimi *et al.* (2014) compare nine rheological models in blood flow simulations in the aortic arch that produce significantly different velocity fields and stress distributions at the walls. This demonstrates how taking the non-Newtonian nature of blood into

consideration can be important, even in regions where the flow velocities are fastest. Other simulations of flow in the coronary arteries show differences in peak pressure values of up to 50% between a Casson-type model and a Newtonian fluid (Apostolidis *et al.* 2016). The chosen rheological model can, moreover, have an effect on the transport of particles (cells and platelets) and can also influence secondary structures that establish themselves (vortex) in the vicinity of arterial stenoses, for example, and that may play a role in the appearance of microembolisms (Buchanan and Kleinstreuer 1998).

#### **1.4.2. Red blood cell aggregation**

In the presence of plasma proteins, red blood cells form aggregates at low shear rates, which are responsible for the shear-thinning nature of the blood mentioned above. The degree of aggregation is directly correlated with the rate of sedimentation of red blood cells, a test commonly used in hematology as a non-specific marker of inflammatory conditions or other blood abnormalities. While immunoglobulin abnormalities, or an abnormal C-reactive protein level associated with an inflammatory response may be associated with a high sedimentation rate, it has been shown that these factors alone are not sufficient to promote aggregation, but are generally associated with an increase in the fibrinogen level, which is considered the main factor of aggregation (Schechner *et al.* 2003; Flormann *et al.* 2015). The flattened shape of red blood cells favors the formation of aggregates in the form of “rouleaux”, similar to stacks of coins (Figure 1.6), which may also agglomerate into aggregates with a less regular shape, or connect to form a network responsible for the existence of a (low) yield stress for blood flow. It should be noted that (reversible) red blood cell aggregation is a fundamentally different phenomenon from (irreversible) coagulation, which leads to the formation of blood clots by polymerizing fibrinogen into a fibrin network, and which represents an important subject of research in itself in view of its biomedical implications (Yeromonahos *et al.* 2010).

Different techniques can be used to characterize aggregation and its structural consequences at the suspension scale: image analysis (Jan and Chien 1973; Chen *et al.* 1994), aggregometry or ektacytometry (Baskurt and Funda 2000; Baskurt *et al.* 2009), light scattering (Shin *et al.* 2005) or acoustic backscatter (Boynard and Lelievre 1990; Franceschini *et al.* 2020) to enable the characterization of the size distribution of aggregates in a flow. While these techniques enable the correlation of aggregate size statistics and

rheology, more local techniques have been used to study microscopic-scale aggregation and disaggregation mechanisms to derive information on underlying mechanisms and characterize cell-scale interaction forces. These include techniques of micropipette aspiration (Buxbaum *et al.* 1982) or atomic force microscopy measurement to determine the interaction energy between two red blood cells in a doublet disaggregation experiment (Steffen *et al.* 2013). Recently, measurements of interaction forces in an aggregation or disaggregation situation have been conducted using multiple optical tweezers, allowing better control of the interaction surface (Yaya 2021).

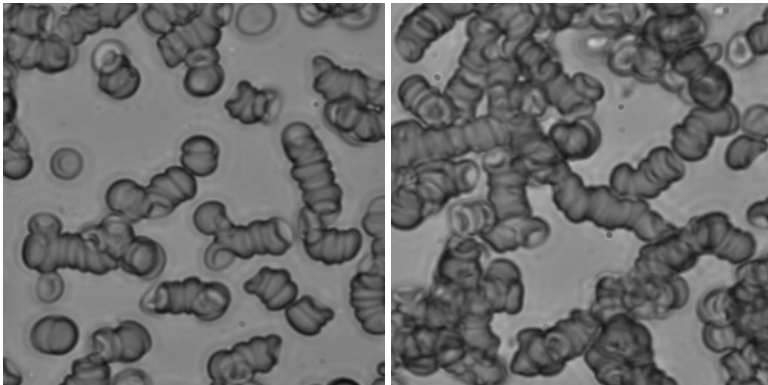


**Figure 1.6.** Aggregates (*rouleaux*) of red blood cells forming an interconnected network. For a color version of this figure, see [www.iste.co.uk/deplano/biological.zip](http://www.iste.co.uk/deplano/biological.zip)

Two mechanisms have been identified to explain aggregation: membrane bridging by aggregation molecules and depletion effects leading to forces of entropic origin. It should be noted that the experimental studies on these mechanisms were not only carried out in solutions containing fibrinogen, the main protein responsible for aggregation under physiological conditions, but also with the help of model molecules such as Dextran, which offers the advantage of existing in a wide range of molecular weights, allowing hypotheses of different theoretical aggregation models to be tested. Historically, the bridging interaction mechanism is the first to have been proposed and is supported by the evidence of macromolecule adsorption on the surface of red blood cells and the role of electrostatic forces (Chien and Jan 1973) to explain the non-monotonous nature of the interaction force as a function of the macromolecular concentration, for which a characteristic bell-shaped curve is generally observed. Models of non-specific interaction have been integrated into numerical simulations of red blood cells in

aggregation (Bagchi *et al.* 2005), based on association and dissociation rates and local ligand concentrations. In the case of fibrinogen, it has also been suggested that specific sites may be involved in adhesive interaction (Lominadze and Dean 2002). Within this context, Pereverzev *et al.* (2005) propose a model in which the receptor-ligand binding can be achieved by two types of bonds, called “slip” and “catch,” the latter being reinforced by the application of a low force. The second mechanism invoked, which is based on depletion effects, was originally proposed by Asakura and Oosawa (1958) and adapted by Neu and Meiselman (2002), to introduce the effects of macromolecular penetration into cell glycocalyx, in order to account for saturation effects responsible for the decrease in interaction at high macromolecular concentrations. In qualitative terms, the depletion effects are related to the finite size of the macromolecules (proteins) in solution, which results in the existence of a steric depletion layer on the surface of the red blood cells. When two red blood cells get close, this exclusion is responsible for a local decrease in the macromolecular concentration within the space separating the two membranes, relative to the concentration in the outer volume. The result is a gradient of concentration and therefore osmolarity, which leads to low pressure in this semi-confined space.

While these two models make it possible to account, at least in qualitative terms and after adjusting the parameters, for the phenomenology of the measurements of interaction energy or forces between red blood cells, questions still remain as to the relative importance of the two phenomena in real systems (fibrinogen, possibly with the synergistic effect linked to other plasma proteins, or dextran in model experiments). In complex situations of red blood cell suspensions in flow, with relative shear motions between membranes, it may be surmised that qualitative differences might have repercussions on the dynamics and mechanisms of aggregation/disintegration under flow. To the extent that only depletion forces are present, these depend only on the instantaneous distance between the red blood cell membranes, regardless of the history of the process. Conversely, a bridging mechanism first involves asymmetry between the aggregation and disaggregation processes from the perspective of the forces involved, all the more so if binding consolidation is established with the contact time. Furthermore, a specific ligand/receptor interaction has implications for the conditions of relative motion of the two membranes in a shear situation, for example. Recent investigations (Yaya 2021) tend to confirm this asymmetry in the force/displacement relationship between aggregation and disaggregation processes when bridging phenomena are involved, which may have repercussions on the stability of aggregates in circulation.

On a microscopic scale and in the absence of hydrodynamic stresses, the morphology of aggregates and their stability are governed by an equilibrium between the attractive or adhesion forces, on the one hand, and the membrane forces on the other. The result, even for the simplest aggregates made up of two cells, is a large variety in morphology, conditioned by the membrane bending energy (Ziherl and Svetina 2007; Flormann *et al.* 2017), as well as the shear modulus of the red blood cell spectrin network, or the differences in size and reduced volume that may result from the dispersity of red blood cell properties within the same sample (Hoore *et al.* 2018).

In flow, a complex interaction occurs between adhesive interaction forces between red blood cells and hydrodynamic effects that tend to both promote aggregation kinetics (by provoking interactions between red blood cells proportional to the local shear rate) and break up existing aggregates (Quemada 1978). Significant efforts have been made in recent years, first, to characterize the aggregate size distributions and their flow dynamics through experimentation, and second, to model aggregation/disaggregation phenomena on a microscopic scale and propose models linking aggregate dynamics, in statistical terms, with blood rheology. The fundamental process in the dynamics of aggregation under flow is that of the interaction between two cells. In modeling terms, this model situation has therefore logically received a certain amount of attention in numerical simulation using several methods. One of the first studies of this type, based on 2D simulations with a front tracking method and a model of a droplet surrounded by a viscoelastic membrane for red blood cells (Bagchi *et al.* 2005) suggests that the rheological properties of cells have a significant effect on stability and aggregate dynamics, with cytoplasmic viscosity and membrane rigidity tending to stabilize aggregates. In this model, the adhesion between cells is modeled by a set of equations reflecting the kinetics of formation and breaking of bonds between the membranes when the distance between them is below a critical distance. Although the authors state that this model does not specifically call on a specific molecular mechanism, it seems more suited to accounting for the effect of a bridging mechanism, rather than a depletion mechanism. Other models use a simple distance-dependent membrane interaction potential of the Morse potential type (Zhang *et al.* 2008; Ju *et al.* 2013) and Lattice–Boltzmann methods (LBM) for fluid dynamics. While qualitative information can be derived regarding the relative effects of adhesion, shear rate or even heterogeneity of red blood cell properties (Ju *et al.* 2013), these models are still limited in quantitative terms and when it comes to comparison with experimental results. Mechanical models of red blood cells remain approximations: neo-Hookean membranes, which do not

offer membrane inextensibility if corrections are not made to the model, and two-dimensional calculations, which cannot account for all of the dynamics and spatial interaction configurations of two red blood cells in a real flow. A similar model has also made it possible to examine the effect of aggregation on the structure and rheology of a red blood cell suspension in a channel (Zhang *et al.* 2009), with the authors notably concluding that aggregation, by making the suspension more compact, tends to increase the depletion layer in the vicinity of the walls (see Figure 1.7 and the following section for a description of this phenomenon) and, counter-intuitively, reduce the apparent viscosity. This influence of aggregation on the depletion layer is confirmed by several experimental studies (Ong *et al.* 2010; Sherwood *et al.* 2012). Other numerical works are based on models such as *coarsened graining* of red blood cells, enabling a large number of objects to be simulated more approximatively, and modeling their aggregation with a Lennard–Jones-type potential (Fedosov *et al.* 2011). While this type of large-scale simulation represents significant progress, allowing a link to be established between microscopic dynamics and rheology, and, notably, experimental viscosity curves to be reproduced (Figure 1.7) as a function of the shear rate or blood yield stress, it should be noted that the nature of the models can at times lead to the mechanical parameter values chosen not necessarily being consistent with the values measured independently or used to simulate other experiments. As a result, microscopic-scale modeling of the phenomena of aggregation under flow is a research pathway that still largely remains to be explored.

Other works suggest a more comprehensive theoretical and statistical approach based on phenomenological kinetic equations modeling the phenomena of aggregation and disaggregation (Chen and Huang 1996), and inclusion of the dynamics of the aggregate network through modeling of energy flows in the system (Kalevotiis and Yanneskis 2011). These models, which require parameter adjustment on experimental data, can represent an interesting intermediate step between microscopic and macroscopic rheological models. Advances in theoretical and numerical modeling of aggregation under flow require and generate experimental developments to characterize the dynamics of aggregation at different scales, from the elementary mechanisms of association and dissociation of red blood cells in aggregates, to the determination of the characteristics and distributions of aggregate sizes in concentrated and complex flows. A number of studies are participating in this effort, based on techniques using imaging (Mehri *et al.* 2014; Kalivotiis *et al.* 2016) or acoustics (Franceschini *et al.* 2020).

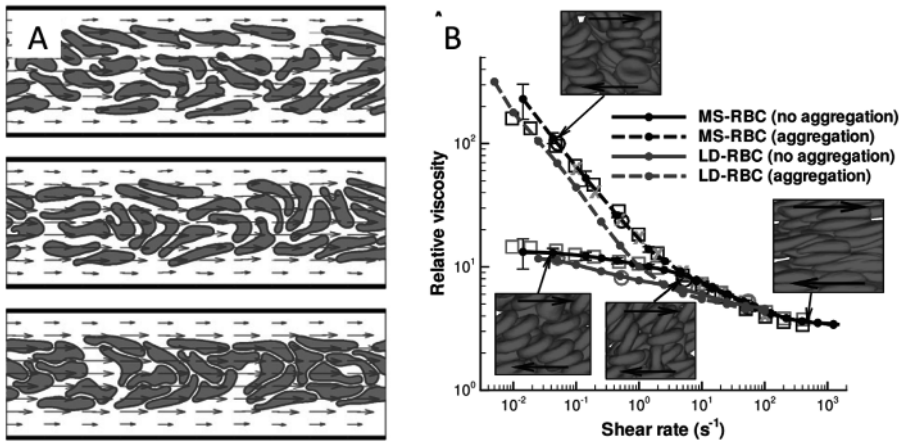


**Figure 1.7.** a) Effect of increasing aggregation (from top to bottom) on the structure of a 2D suspension of red blood cells (from Zhang *et al.* (2009)). b) Experimental and simulated rheology of a suspension of shear red blood cells. Open symbols: experimental data; solid lines: mesoscopic model (MS-RBC); dashed lines: low-dimensionality model (LD-RBC) (according to Fedosov *et al.* (2011)). For a color version of this figure, see [www.iste.co.uk/deplano/biological.zip](http://www.iste.co.uk/deplano/biological.zip)

Rheological data (see Figure 1.5) and mean shear rate values in capillaries (of the order of  $1,000 \text{ s}^{-1}$ ) have long meant that aggregation can only play a role in the center of larger vessels (arteries, veins, venules and possibly arterioles), where shear rates are relatively lower. Trains of cells (clusters) are observed in capillaries *in vivo*, however, with their formation and stabilization mechanisms forming the subject of several recent studies (see Figure 1.8(a)). While it is recognized that these clusters of cells can form and even be stabilized by hydrodynamic interaction processes (Claveria *et al.* 2016), experimental and numerical studies have shown that there is a strong correlation between the probability of these clusters occurring and the concentration of the aggregating agent (dextran or fibrinogen), in ranges of concentration (and thus interaction energy) that may cover physiological ranges in healthy or pathological situations (Brust *et al.* 2014). With aggregation tending to stabilize red blood cell clusters in capillaries, aggregation is likely to play a role in microcirculation through local changes in flow resistance, and more generally in red blood cell behavior in microcirculation networks.

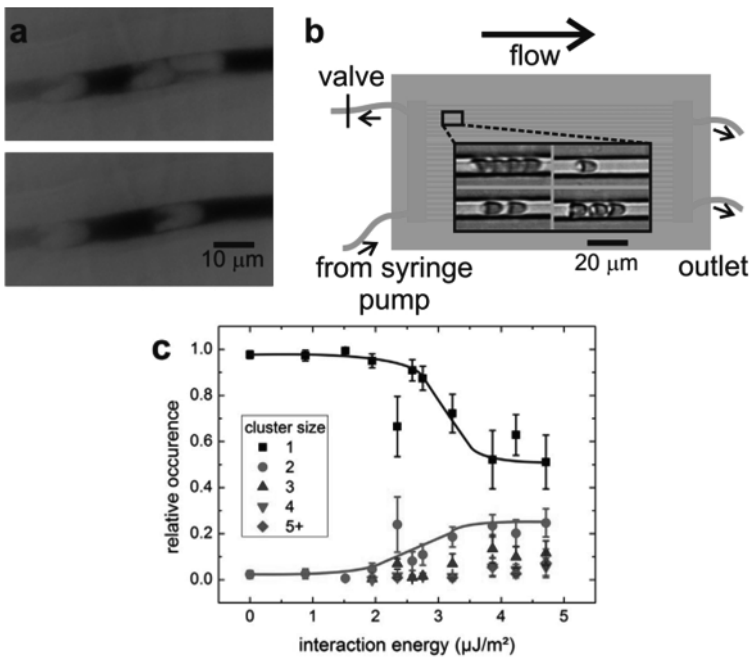


**Figure 1.8.** *a)* Red blood cell flow in a mouse capillary, showing both isolated blood cells and groups of cells potentially in adhesion. *b)* Study in microfluidic channels of the role of aggregation on the size of groups of red blood cells. *c)* Statistics of aggregate sizes as a function of interaction energy (controlled by Dextran or fibrinogen concentration (Brust et al. 2014)). For a color version of this figure, see [www.iste.co.uk/deplano/biological.zip](http://www.iste.co.uk/deplano/biological.zip)

### 1.4.3. Dynamics of microcirculation

In the systemic circulation, between the arterial system that conveys a highly pulsed flow of oxygenated blood from the heart and the venous system that brings it back to the heart, lies the domain of microcirculation, consisting of vessels whose diameter is less than a few hundred micrometers. These regions of the vascular system consist of complex networks of vessels, the finest of which, the capillaries, have a diameter of 4–8  $\mu\text{m}$ , are preceded by arterioles and are followed by venules. The largest part of the pressure drop between leaving the heart through the aorta and returning through the vena cava occurs in these dense, branched networks, which irrigate all of the organs. The boundary conditions of the transport in large vessels are therefore determined by the resistance imposed by microcirculation, which,

moreover, is a system regulated by mechanisms of vasodilatation or vasoconstriction responding to local supply needs for oxygen, heat or immune response, for example. Indeed, it is in the microcirculation that the blood functions are manifested, and the walls of the arterioles are sensitive to shear stresses on the wall and can activate contractile cells, enabling the flow in the capillaries to be regulated. Significant, repeated variations of these wall stresses can also trigger an adaptation of the vessels (vascular remodeling) and the capillary network (angiogenesis).

The fundamental difference in the nature of flow between microcirculation and macrocirculation (large vessels) is not limited to differences in the order of magnitude of the characteristic numbers (Reynolds number and Womersley number). These aspects are certainly crucial: flows are dominated here by viscous effects, and fluid dynamics can generally be modeled by the Stokes equation at these scales. Cardiac pulsations are markedly dampened here, ensuring quasi-stationary conditions, but the scale of the flows also means that blood does not behave as a uniform continuous medium here, with its nature as a dense suspension of deformable particles giving rise to specific phenomena. In arterioles or venules, the vessel diameter is less than 30 times the diameter of a red blood cell, and in the finest capillaries, the red blood cells even have to deform to pass through a conduit smaller than their own diameter. The structure and rheology of the suspension are therefore dominated by cell–cell and cell–wall interactions, and depart significantly from the rheological laws applicable in large vessels or viscometric flows.

The structural characteristics of microcirculatory flows, revealed by Poiseuille (1835), can be seen in Figure 1.9, which shows his representation of the microvascular network of the frog mesentery and circulating red blood cells. Two observations stand out: (i) in the precapillary arterioles and postcapillary venules there is a depletion layer with no red blood cells in the vicinity of the walls, generally called the cell-free layer (CFL); (ii) the red blood cell distribution is very heterogeneous in the capillaries and the hematocrit is not homogeneous. More recent imaging techniques are able to confirm these observations and record network geometries useful for simulating blood flow models based, for example, on effective rheological laws and phase separation laws at the bifurcations responsible for the heterogeneities observed.

The non-uniform distribution of red blood cells in the cross-section of a vessel and the existence of a depletion layer (CFL) at the walls are responsible for two significant rheological effects in blood flows in a tube. The first, identified by Fåhræus, indicates that for a given systemic hematocrit, the apparent hematocrit in the microcirculation is less than the hematocrit of the reservoir that supplies it (artery), and decreases with the diameter of the vessels. This is a consequence of the conservation of red blood cell and plasma flows, and because the blood cells are on average more centered in the channel than the plasma, as their velocity is greater. A correlation between tube hematocrit, discharge (or reservoir) hematocrit and vessel diameter is proposed by Pries *et al.* (1990). The second effect correlated with the existence of the cell-free marginal layer is the Fåhræus–Lindqvist effect, which consists of a decrease in the apparent viscosity of the blood when the tube diameter decreases. This counterintuitive effect is the result of the lubricating effect of the marginal layer, whose viscosity (that of plasma) is lower than that of the dense suspension flowing through the middle of the channel (Fåhræus and Lindqvist 1931).

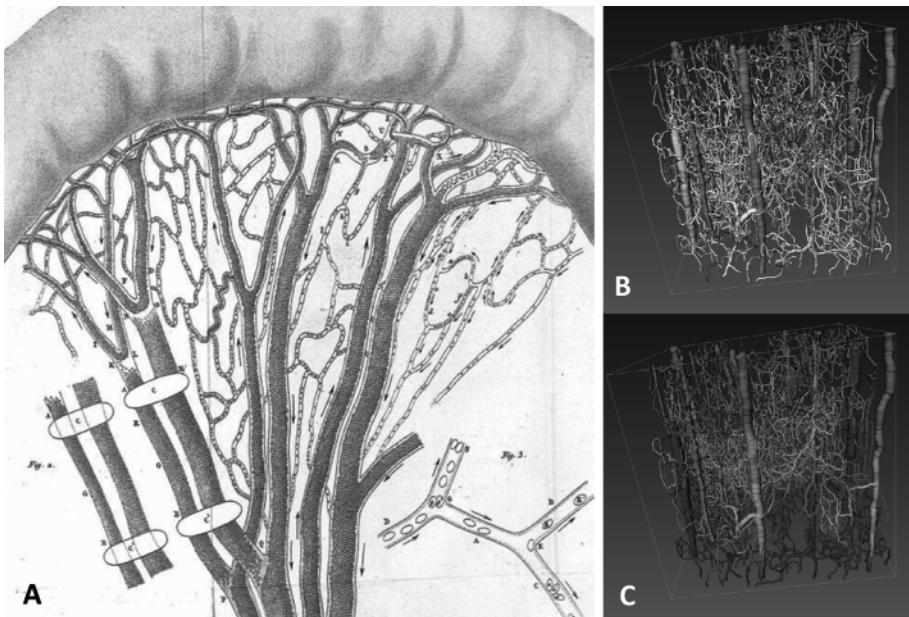


**Figure 1.9.** Microcirculation networks: (a) frog mesentery (Poiseuille 1835); (b and c) color-coded representations of simulated fields (b: hematocrit, c: flow) in a network geometry acquired by X-ray tomography in monkey brain (Guibert *et al.* 2010). Scale bar: 500  $\mu\text{m}$

On a microscopic scale, the structuring of the suspension responsible for these phenomena is governed by two antagonistic processes, which are, first, a migration of cells away from the walls and toward the center of the channel, and second, a shear-induced diffusion and interactions between red blood cells. These processes, which are common to all suspensions of deformable objects, have become the subject of works permitting scaling laws to be proposed (Podgorski *et al.* 2011; Grandchamp *et al.* 2013; Losserand *et al.* 2019), and are strongly influenced by the mechanical properties of circulating cells, which can make them tools of interest for diagnosis, indirect characterization of these properties or cell sorting (Geislinger and Franke 2013; Connolly *et al.* 2021). In a polydisperse system, such as blood, this sensitivity to cell properties also leads to margination and segregation phenomena, where the most rigid and smallest cells tend to be closer to the walls (white blood cells, platelets and, potentially, more rigid pathological red blood cells), on average. While there are continuous models to describe margination, as well as numerical works (Kumar and Graham 2012), the details of the mechanisms remain the subject of active research. There has been a renewed international interest in this subject among teams of theorists/numerical analysts, further to the evolution of numerical models and computing means (Fedosov and Gompper 2014; Qi and Shaqfeh 2017), underscoring a need for quantitative experimental data.

The heterogeneity of the distribution of hematocrit visible in Figure 1.9 is a consequence of the asymmetric separation of red blood cells in the network bifurcations. Model experiments in microfluidics have shown that in general, for perfectly symmetrical bifurcations where the two outlet branches are geometrically identical, if the flow rates are different in these two branches (e.g. because the outlet pressures or branch lengths are different), the red blood cell volume fraction (hematocrit) is higher in the branch of higher flow rate. This phenomenon, widely observed in microcirculation, is generally referred to as the Zweifach–Fung effect (Svanes and Zweifach 1968; Fung 1973). Under physiological conditions, it can be estimated that if the asymmetry of the bifurcation outlet flow rates is such that one branch receives only a quarter of the inlet flow rate, the hematocrit in that branch may fall to zero. There have been a large number of *in vivo* studies devoted to this phenomenon (Pries *et al.* 1996), as well as studies on model systems (Chien *et al.* 1985) or numerical simulations (Barber *et al.* 2008). The phenomenon is relatively subtle, and strongly depends on the configuration of the particles or blood cells that arrive at the bifurcation (Doyeux *et al.* 2011), which may even lead to the inversion of the partition in some cases (Shen *et al.* 2015). These effects, coupled with the dynamics of the

reorganization of red blood cells in the network branches between two bifurcations, under the effect of the migration/diffusion mechanisms mentioned above, are crucial for the distribution of red blood cells at the scale of a capillary network (Balogh and Bagchi 2018).

The strong coupling between (i) the structure of the suspension in the network branches, (ii) the apparent viscosity in these branches and (iii) the phase separation at the bifurcations cannot only lead to heterogeneities in the hematocrit distribution, but also to spatiotemporal fluctuations in the flow (Kiani *et al.* 1994). The oscillations and instabilities of microvascular flows have been observed in vivo (Mezentseva *et al.* 2016) and are suspected to have an impact on the regulation of blood flow and tissue oxygenation. To date, the question of the stability of these flows has formed the subject of some recent theoretical studies, but there is very little experimental validation (Davis and Pozrikidis 2014; Karst *et al.* 2017), making it a relatively active subject of study aimed at clarifying the purely passive mechanisms of microcirculation regulation. The inclusion of effects related to aggregation, its influence on red blood cell distribution and blood perfusion in the capillary networks is also an active research topic (Reinhart 2017; Kaliviotis *et al.* 2018).

## 1.5. Conclusion

According to the WHO, cardiovascular disease, affecting the circulatory system, is the leading cause of mortality worldwide, accounting for more than 30% of deaths, predominantly from coronary heart disease and strokes. In addition, hemopathies, which affect the components of the blood, constitute a group of diseases, many of which hereditary, that are highly prevalent. While the causes, mechanisms and consequences of these pathologies are extremely varied and affect different circulation levels, a common characteristic discussed in this chapter is their fundamentally multi-scale nature, coupling biology and physicochemistry, circulating cell mechanics and vascular walls, blood rheology and hydrodynamics at vessel and circulatory-network scale.

The quantitative understanding and modeling of the physical and mechanical aspects of blood circulation dynamics continue to represent a challenge related to its nonlinear character and extreme sensitivity to biomechanical and physicochemical parameters, which are likely to vary greatly in pathological cases. The past few decades have seen significant

developments in both in vivo and in vitro experimental techniques (optical and acoustic imaging and Magnetic Resonance Imaging). There have also been advances in numerical simulation, in terms of both methods and computing power, which now allow the study of large systems with a multiphysics approach. As a result, considerable progress has been made in understanding the rheological properties of blood and circulatory dynamics. In addition to a better fundamental understanding of hemodynamics and hemorrheology, these advances offer new scope for fruitful interactions at the interface between medicine, physics and mechanics in areas such as diagnosis, patient monitoring assistance and preoperative decision support within the framework of vascular surgery, because of the ever-increasing predictive ability of the models.

## 1.6. References

- Apostolidis, A.J., Moyer, A.P., Beris, A.N. (2016). Non-Newtonian effects in simulations of coronary arterial blood flow. *J. of Non-Newtonian Fluid Mech.*, 233, 155–165.
- Asakura, S. and Oosawa, F. (1958). Interaction between particles suspended in solutions of macromolecules. *J. Polym. Sci.*, 33, 183–192.
- Asakura, T., Mattiello, J.A., Obata, K., Asakura, K., Reilly, M.P., Tomassini, N., Schwartz, E., Ohene-Frempong, K. (1994). Partially oxygenated sickled cells: Sickle-shaped red cells found in circulating blood of patients with sickle cell disease. *Proc. Nat. Acad. Sci.*, 91, 1–5.
- Bagchi, P., Johnson, P.C., Popel, A.S. (2005). Computational fluid dynamic simulation of aggregation of deformable cells in a shear flow. *Biochem. Eng. J.*, 127, 1070–1080.
- Ballyk, P.D., Steinman, D.A., Ethier, C.R. (1994). Simulation of non-Newtonian blood flow in an end-to-end anastomosis. *Biorheology*, 31(5), 565–586.
- Balogh, P. and Bagchi, P. (2018). Analysis of red blood cell partitioning at bifurcations in simulated microvascular networks. *Phys. Fluids*, 30, 051902.
- Barabino, G.A., Platt, M.O., Kaul, D.K. (2010). Sickle cell biomechanics. *Annu. Rev. Biomed. Eng.*, 12, 345–367.
- Barber, J.O., Alberding, J.P., Restrepo, J.M., Secomb, T.W. (2008). Simulated two-dimensional red blood cell motion, deformation, and partitioning in microvessel bifurcations. *Ann. Biomech. Engng.*, 36, 1690–1698.

- Baskurt, O.K. and Funda, M. (2000). Importance of measurement temperature in detecting the alterations of red blood cell aggregation and deformability studied by ektacytometry: A study on experimental sepsis in rats. *Clin. Hemorheol. Microcirc.*, 23, 43–49.
- Baskurt, O.K., Uyuklu, M., Ulker, P., Cengiz, M., Nemeth, N., Alexy, T., Shin, S., Hardeman, M.R., Meiselman, H.J. (2009). Comparison of three instruments for measuring red blood cell aggregation. *Clin. Hemorheol. Microcirc.*, 43, 283–298.
- Betz, T., Lenz, M., Joanny, J.-F., Sykes, C. (2009). ATP-dependent mechanics of red blood cells. *Proc. Nat. Acad. Sci.*, 106, 15320–15325.
- Biben, T., Farutin, A., Misbah, C. (2011). Three-dimensional vesicles under shear flow: Numerical study of dynamics and phase diagram. *Phys. Rev. E.*, 83, 031921.
- Bird, R.B., Armstrong, R.C., Hassager, O. (1987). *Dynamics of Polymeric Liquids*, 2nd edition. Wiley, New York.
- Bosch, F.H., Werre, J.M., Roerdinkholder-Stoelwinder, B., Huls, T.H., Willekens, F.L., Halie, M.R. (1992). Characteristics of red blood cell populations fractionated with a combination of counterflow centrifugation and percoll separation. *Blood*, 79, 254–260.
- Boynard, M. and Lelievre, J.C. (1990). Size determination of red blood cell aggregates induced by dextran using ultrasound backscattering phenomenon. *Biorheology*, 27, 39–46.
- Brust, M., Aouane, O., Thiébaud, M., Flormann, D., Verdier, C., Kaestner, L., Laschke, M. W., Selmi, H., Benyoussef, A., Podgorski, T., Coupier, G., Misbah, C., Wagner, C. (2014). The plasma protein fibrinogen stabilizes clusters of red blood cells in micro capillary flows. *Sci. Rep.*, 4, 4348.
- Buchanan, J.R. and Kleinstreuer, C. (1998). Simulation of particle-hemodynamics in a partially occluded artery segment with implications to the initiation of microemboli and secondary stenoses. *J Biomech Eng.*, 120(4), 446–454.
- Buchanan, J.R., Kleinstreuer, C., Comer, J.K. (2000). Rheological effects on pulsatile hemodynamics in a stenosed tube. *Computers & Fluids*, 20, 695–724.
- Buxbaum, K., Evans, E., Brooks, D.E. (1982). Quantitation of surface affinities of red blood cells in dextran solutions and plasma. *Biochemistry*, 21, 3235–3239.
- Chen, J. and Huang, Z. (1996). Analytical model for effects of shear rate on rouleau size and blood viscosity. *Biophys. Chem.*, 58, 273–279.

- Chen, S., Barshtein, G., Gavish, B., Mahler, Y., Yedgar, S. (1994). Monitoring of red blood cell aggregability in a flow-chamber by computerized image analysis. *Clin. Hemorheol.*, 14, 497–508.
- Chien, S. (1970). Shear dependence of effective cell volume as a determinant of blood viscosity. *Science*, 168, 977–979.
- Chien, S. and Jan, K.M. (1973). Red cell aggregation by macromolecules: Roles of surface adsorption and electrostatic repulsion. *J. Supramol. Struct.*, 1, 385–409.
- Chien, S., Tvetenstrand, C.D., Epstein, M.A., Schmid-Schonbein, G.W. (1985). Model studies on distributions of blood cells at microvascular bifurcations. *Am. J. Physiol. Heart Circ. Physiol.*, 248, H568–H576.
- Cho, Y.I. and Kensey, K.R. (1991). Effects of the non-Newtonian viscosity of blood on flows in a diseased arterial vessel. Part 1: Steady flows. *Biorheology*, 28, 241–262.
- Claveria, V., Aouane, O., Thiébaud, M., Abkarian, M., Coupier, G., Misbah, C., John, T., Wagner, C. (2016). Clusters of red blood cells in microcapillary flow: Hydrodynamic versus macromolecule induced interaction. *Soft Matter*, 12, 8235–8245.
- Connes, P., Simmonds, M.J., Brun, J.-F., Baskurt, O. (2013). Exercise hemorheology: Classical data, recent findings and unresolved issues. *Clin. Hemorheol. Microcirc.*, 53, 187–199.
- Connolly, S., McGourty, K., Newport, D. (2021). The influence of cell elastic modulus on inertial positions in poiseuille microflows. *Biophys. J.*, 120, 855–865.
- Cordasco, D. and Bagchi, P. (2014). Intermittency and synchronized motion of red blood cell dynamics in shear flow. *J. Fluid Mech.*, 759, 472–488.
- Da Costa, L., Galimand, J., Fenneteau, O., Mohandas, N. (2013). Hereditary spherocytosis, elliptocytosis, and other red cell membrane disorders. *Blood Rev.*, 27(4), 167–178.
- Davis, J.M. and Pozrikidis, C. (2014). Self-sustained oscillations in blood flow through a honeycomb capillary network. *Bull. Math. Biol.*, 76, 2217–2237.
- Dintenfass, L. (1962). Thixotropy of blood and proneness to thrombus formation. *Circ. Res.*, 11, 233–239.
- Doyeux, V., Podgorski, T., Peponas, S., Ismail, M., Coupier, G. (2011). Spheres in the vicinity of a bifurcation: Elucidating the Zweifach–Fung effect. *J. Fluid Mech.*, 674, 359–388.
- Dupire, J., Socol, M., Viallat, A. (2012). Full dynamics of a red blood cell in shear flow. *Proc. Nat. Acad. Sci. USA*, 109, 20808–20813.

- Evans, E. and Fung, Y.-C. (1972). Improved measurements of the erythrocyte geometry. *Microvasc. Res.*, 4, 335–347.
- Fåhræus, R. and Lindqvist, T. (1931). The viscosity of the blood in narrow capillary tubes. *Am. J. Physiol.*, 96, 562–568.
- Fedosov, D.A. and Gompper, G. (2014). White blood cell margination in microcirculation. *Soft Matter*, 10, 2961–2970.
- Fedosov, D.A., Pan, W., Caswell, B., Gompper, G., Karniadakis, G.E. (2011). Predicting human blood viscosity in silico. *Proc. Nat. Acad. Sci.*, 108, 11772–11777.
- Fischer, T.M. and Korzeniewski, R. (2013). Threshold shear stress for the transition between tumbling and tank-treading of red blood cells in shear flow: Dependence on the viscosity of the suspending medium. *J. Fluid Mech.*, 736, 351–365.
- Flormann, D., Kuder, E., Lipp, P., Wagner, C., Kaestner, L. (2015). Is there a role of C-reactive protein in red blood cell aggregation? *Int. J. Laboratory Hematology*, 37(4), 474–482.
- Flormann, D., Aouane, O., Kaestner, L., Ruloff, C., Misbah, C., Podgorski, T., Wagner, C. (2017). The buckling instability of aggregating red blood cells. *Sci. Rep.*, 7, 7928.
- Franceschini, E., Yu, F.T.H., Destrempes, F. (2020). Ultrasound characterization of red blood cell aggregation with intervening attenuating tissue-mimicking phantoms. *J. Acoust. Soc. Amer.*, 127, 1104–1115.
- Fung, Y.C. (1973). Stochastic flow in capillary blood vessels. *Microvasc. Res.*, 5, 34–48.
- Fung, Y.C. (1993). *Biomechanics: Mechanical Properties of Living Tissues*, 2nd edition. Springer, Berlin.
- Geddes, J.B., Carr, R.T., Karst, N.J., Wu, F. (2007). The onset of oscillations in microvascular blood flow. *SIAM J. Appl. Dyn. Syst.*, 6, 694.
- Geislinger, T. and Franke, T. (2014). Hydrodynamic lift of vesicles and red blood cells in flow – From Fåhræus and Lindqvist to microfluidic cell sorting. *Adv. Coll. Interface Sci.*, 208, 161–176.
- Grandchamp, X., Coupier, G., Srivastav, A., Minetti, C., Podgorski, T. (2013). Lift and down-gradient shear-induced diffusion in red blood cell suspensions. *Phys. Rev. Lett.*, 110, 108101.
- Guibert, R., Fonta, C., Plouraboué, F. (2010). Cerebral blood flow modeling in primate cortex. *J. Cerebral Blood Flow and Metabolism*, 30, 1860–1873.

- Hales, S. (1733). *Statistical Essays: Containing Haemastaticks*. Innys, Manby & Woodward, London.
- Harvey, W. and Leake, C.D. (1928). *Exercitatio Anatomica de Motu Cordis and Sanguinis in Animalibus*. Facsimile of the original Latin ed. (1628) and English translation. Charles C. Thomas, Springfield.
- Hawkey, C.M. (1975). *Comparative Mammalian Haematology*. Butterworth-Heinemann, Elsevier, Oxford.
- Helfrich W. (1973). Elastic properties of lipid bilayers: Theory and possible experiments. *Z. Naturforsch.*, 28, 693–703.
- Higgs, D.R., Engel, J.D., Stamatoyannopoulos, G. (2012). Thalassaemia. *Lancet*, 379, 373–383.
- Hoore, M., Yaya, F., Podgorski, T., Wagner, C., Gompper, G., Fedosov, D.A. (2018). Effect of spectrin network elasticity on the shapes of erythrocyte doublets. *Soft Matter*, 14, 6278–6289.
- Jan, K.M. and Chien, S. (1973). Role of surface electric charge in red blood cell interactions. *J. Gen. Phys.*, 61, 638–654.
- Jensen, K.H., Kim, W., Holbrook, N.M., Bush, J.M.W. (2013). Optimal concentration in transport systems. *J. R. Soc. Interface*, 10, 20130138.
- Ju, M., Ye, S.S., Low, H.T., Zhang, J., Cabrales, P., Leo, H.L., Kim, S. (2013). Effect of deformability difference between two erythrocytes on their aggregation. *Phys. Biol.*, 10, 036001.
- Kaliviotis, E. and Yianneskis, M. (2011). Blood viscosity modelling: Influence of aggregate network dynamics under transient conditions. *Biorheology*, 48, 127–147.
- Kaliviotis, E., Dusing, J., Sherwood, J.M., Balabani, S. (2016). Quantifying local characteristics of velocity, aggregation and hematocrit of human erythrocytes in a microchannel flow. *Clin. Hemorheol. Microcirc.*, 63, 123–148.
- Kaliviotis, E., Sherwood, J.M., Balabani, S. (2018). Local viscosity distribution in bifurcating microfluidic blood flows. *Phys. Fluids*, 30, 030706.
- Karimi, S., Dabagh, M., Vasava, P., Dadvar, M., Dabir, B., Jalali, P. (2014). Effect of rheological models on the hemodynamics within human aorta: CFD study on CT image-based geometry. *J. Non-Newtonian Fluid Mech.*, 207, 42–52.
- Karst, N.J., Geddes, J.B., Carr, R.T. (2017). Model microvascular networks can have many equilibria. *Bull. Math. Biol.*, 79, 1–20.
- Kelemen, C., Chien, S., Artmann, G.M. (2001). Temperature transition of human hemoglobin at body temperature: Effects of calcium. *Biophys. J.*, 80, 2622–2630.

- Kiani, M.F., Pries, A.R., Hsu, L.L., Sarelius, I.H., Cokelet, G.R. (1994). Fluctuations in microvascular blood flow parameters caused by hemodynamic mechanisms. *Am. J. Physics*, 266, H1822.
- Ku, D.N. (1997). Blood flow in arteries. *Annu. Rev. Fluid Mech.*, 29, 399–434.
- Kumar, A. and Graham, M.D. (2012). Margination and segregation in confined flows of blood and other multicomponent suspensions. *Soft Matter*, 8, 10536–10548.
- Kumar, V., Abbas, A.K., Aster, J.C. (2012). *Robbins Basic Pathology*, 9th edition. Saunders, Philadelphia.
- Lac, E. and Barthès-Biesel. D. (2005). Deformation of a capsule in simple shear flow: Effect of membrane prestress. *Phys. Fluids*, 17, 072105.
- Lanotte, L., Mauer, J., Mendez, S., Fedosov, D.A., Fromental, J.-M., Claveria, V., Nicoud, F., Gompper, G., Abkarian, M. (2016). Red cells dynamic morphologies govern blood shear thinning under microcirculatory flow conditions. *Proc. Natl. Acad. Sci. USA*, 113, 13289–13294.
- Lee, S.W. and Steinman, D.A. (2007). On the relative importance of rheology for image-based CFD models of the carotid bifurcation. *J. Biomed. Engrg. – Trans. ASME*, 129, 273–278.
- Levant, M. and Steinberg, V. (2016). Intermediate regime and a phase diagram of red blood cell dynamics in a linear flow. *Phys. Rev. E*, 94, 062412.
- Lewis, J.H. (1996). *Comparative Hemostasis in Vertebrates*. Plenum Publishing Co., New York.
- Linderkamp, O., Friederichs, E., Boehler, R., Ludwig, A. (1993). Age dependency of red blood cell deformability and density: Studies in transient erythroblastopenia of childhood. *British J. Haematol.*, 83, 125.
- Lominadze, D. and Dean, W.L. (2002). Involvement of fibrinogen specific binding in erythrocyte aggregation. *FEBS Lett.*, 517, 1–3.
- Losserland, S., Coupier, G., Podgorski, T. (2019). Migration velocity of red blood cells in microchannels. *Microvasc. Res.*, 124, 30–36.
- Mauer, J., Mendez, S., Lanotte, L., Nicoud, F., Abkarian, M., Gompper, G., Fedosov, D.A. (2018). Flow-induced transitions of red blood cell shapes under shear. *Phys. Rev. Lett.*, 121, 118103.
- McMillan, D.E., Utterback, N.G., Nasrinasrabadi, M., Lee, M.M. (1986). An instrument to evaluate the time dependent flow properties of blood at moderate shear rates. *Biorheology*, 23, 63–74.

- Mehri R., Laplante, J., Mavriplis, C., Fenech, M. (2014). Investigation of blood flow analysis and red blood cell aggregation. *J. Med. Biol. Eng.*, 34, 469–474.
- Mezentseva, L.V., Pertsov, S.S., Hugaeva, V.K. (2016). A comparative analysis of the persistence of capillary blood flow oscillations in the left and right rat kidneys. *Biophysics*, 61, 656.
- Minetti, C., Audemar, V., Podgorski, T., Coupier, T. (2019). Dynamics of a large population of red blood cells under shear flow. *J. Fluid Mech.*, 864, 408–448.
- Nagel, R.L., Fabry, M.E., Steinberg, M.H. (2003). The paradox of hemoglobin SC disease. *Blood Reviews*, 17, 167–178.
- Neu, B. and Meiselman, H.J (2002). Red blood cell aggregation in polymer solutions. *Biophys. J.*, 83, 2482–2490.
- Ong, P.K., Namgung, B., Johnson, P.C., Kim, S. (2010). Effect of erythrocyte aggregation and flow rate on cell-free layer formation in arterioles. *Am. J. Physiol. Heart Circ. Physiol.*, 298, H1870–H1878.
- Park, Y., Best, C.A., Auth T., Gov, N.S., Safran, S.A., Popescu, G., Suresh, S., Feld, M.S. (2010). Metabolic remodeling of the human red blood cell membrane. *Proc. Natl. Acad. Sci. USA*, 107, 1289–1294.
- Peng, Z., Mashayekh, A., Zhu, Q. (2014). Erythrocyte responses in low-shear-rate flows: Effects of non-biconcave stress-free state in the cytoskeleton. *J. Fluid Mech.*, 742, 96–118.
- Pereverzev, Y.V., Prezhdo, O.V., Forero, M., Sokurenko, E.V., Thomas, W.E. (2005). The two-pathway model for the catch-slip transition in biological adhesion. *Biophys. J.*, 89, 1446–1454.
- Picart, C., Piau, J.-M., Gaillard, H., Carpentier, P. (1998). Human blood shear yield stress and its hematocrit dependence. *J. Rheol.*, 42, 1–12.
- Podgorski, T., Callens, N., Minetti, C., Coupier, G., Dubois, F., Misbah, C. (2011). Dynamics of vesicle suspensions in shear flow between walls. *Microgravity Sci. Technol.*, 23, 263–270.
- Poiseuille, J.-L.-M. (1835). *Recherches sur les causes du mouvement du sang dans les vaisseaux capillaires*. Imprimerie Royale, Paris.
- Poiseuille, J.-L.-M. (1844). *Recherches experimentales sur le mouvement des liquides dans les tubes de tres-petits diametres*. Imprimerie Royale, Paris.
- Pries, A.R., Secomb, T.W., Gaehtgens, P., Gross, J.F. (1990). Blood flow in microvascular networks: Experiments and simulation. *Circ. Res.*, 67, 826–834.

- Pries, A.R., Secomb, T.W., Gaethgens, P. (1996). Biophysical aspects of blood flow in the microvasculature. *Cardiovasc. Res.*, 32, 654–667.
- Qi, Q.M. and Shaqfeh, S.G. (2017). Theory to predict particle migration and margination in the pressure-driven channel flow of blood. *Phys. Rev. Fluids*, 2, 093102.
- Quemada, D. (1978). Rheology of concentrated disperse systems II. A model for non-Newtonian shear viscosity in steady flows. *Rheol. Acta*, 17, 632–642.
- Rees, D.C., Williams, T.N., Gladwin, M.T. (2010). Sickle-cell disease. *Lancet*, 376, 2018–2031.
- Reinhart, W.H. (2016). The optimum hematocrit. *Clin. Hemorheol. Microcirc.*, 64, 575–585.
- Reinhart, W.H., Piety, N.Z., Shevkopyas, S.S. (2017). Influence of red blood cell aggregation on perfusion of an artificial microvascular network. *Microcirculation*, 24, e12371.
- Reitsma, S., Slaaf, D.W., Vink, H., van Zandvoort, M.A.M.J., oude Egbrink, M.G.A. (2017). The endothelial glycocalyx: Composition, functions, and visualization. *Pflügers Arch – Eur. J. Physiol*, 454, 345–359.
- Ross, P.D. and Minton, A.P. (1977). Hard quasispherical model for the viscosity of hemoglobin solutions. *Biochem. Biophys. Res. Comm.*, 76, 971–976.
- Schechner, V., Shapira, I., Berliner, S., Comaneshter, D., Hershcovici, T., Orlin, J., Zeltser, D., Rozenblat, M., Lachmi, K., Hirsch, M., Beigel, Y. (2003). Significant dominance of fibrinogen over immunoglobulins, C-reactive protein, cholesterol and triglycerides in maintaining increased red blood cell adhesiveness/aggregation in the peripheral venous blood: A model in hypercholesterolaemic patients. *Eur. J. Clin. Invest.*, 33, 955–961.
- Seguin, B. and Fried, E. (2014). Microphysical derivation of the Canham–Helfrich free-energy density. *J Math. Biol.*, 68, 647–665.
- Shen, Z., Coupier, G., Kaoui, B., Polack, B., Harting, J., Misbah, C., Podgorski, T. (2015). Inversion of hematocrit partition at microfluidic bifurcations. *Microvasc. Res.*, 105, 40–46.
- Sherwood, J.M., Dusting, J., Kaliviotis, E., Balabani, S. (2012). The effect of red blood cell aggregation on velocity and cell-depleted layer characteristics of blood in a bifurcating microchannel. *Biomicrofluidics*, 6, 024119.
- Shin, S., Ku, Y., Park, M.-S., Suh, J.-S. (2005). Slit-flow ektacytometry: Laser diffraction in a slit rheometer. *Cytom. Part B: Clin. Cy.*, 65B, 6–13.

- Sinha, K. and Graham, M.D. (2015). Dynamics of a single red blood cell in simple shear flow. *Phys. Rev. E*, 92, 042710.
- Steffen, P., Verdier, C., Wagner, C. (2013). Quantification of depletion-induced adhesion of red blood cells. *Phys. Rev. Lett.*, 110, 018102.
- Stoltz, J.F. and Lucius, M. (1981). Viscoelasticity and thixotropy of human blood. *Biorheology*, 18, 453–473.
- Svanes, K. and Zweifach, B.W. (1968). Variations in small blood vessel hematocrits produced in hypothermic rats by micro-occlusion. *Microvasc. Res.*, 1, 210–220.
- Švelc, T. and Svetina, S. (2012). Stress-free state of the red blood cell membrane and the deformation of its cytoskeleton. *Cell. Mol. Biol. Lett.*, 17, 217–227.
- Thurston, G.B. (1973). Frequency and shear rate dependence of viscoelastic of human blood. *Biorheology*, 10(3), 375–381.
- Tomaiuolo, G. (2014). Biomedical properties of red blood cells in health and disease toward microfluidics. *Biomicrofluidics*, 8, 051501.
- Varchanis, S., Dimakopoulos, Y., Wagner, C., Tsamopoulos, J. (2018). How viscoelastic is human blood plasma? *Soft Matter*, 14, 4238–4251.
- Vlahovska, P.M., Podgorski, T., Misbah, C. (2009). Vesicles and red blood cells in flow: From individual dynamics to rheology. *C. R. Physique*, 10, 775–789.
- Wan, J., Forsyth, A.M., Stone, H.A. (2011). Red blood cell dynamics: From cell deformation to ATP release. *Integr. Biol.*, 3, 972–981.
- Weber, C. and Noels, H. (2011). Atherosclerosis: Current pathogenesis and therapeutic options. *Nat. Med.*, 17, 1410–1422.
- Weed, R.I., LaCelle, P.L., Merrill, E.W. (1969). Metabolic dependence of red cell deformability. *J. Clin. Invest.*, 48, 795–809.
- Weinbaum, S., Tarbell, J.M., Damiano, E.R. (2007). The structure and function of the endothelial glycocalyx layer. *Annu. Rev. Biomed. Eng.*, 9, 121–167.
- Yaya, F. (2021). Physical properties of red blood cells in aggregation. PhD Thesis, Universität des Saarlandes, Saarbücken and Université Grenoble Alpes, Grenoble.
- Yeromonahos, C., Polack, B., Caton, F. (2010). Nanostructure of the fibrin clot. *Biophys. J.*, 99, 2018–2027.
- Zhang, J., Johnson, P.C., Popel, A. (2008). Red blood cell aggregation and dissociation in shear flows simulated by lattice Boltzmann method. *J. Biomech.*, 41, 47–55.

- Zhang, J., Johnson, P.C., Popel, A. (2009). Effects of erythrocyte deformability and aggregation on the cell free layer and apparent viscosity of microscopic blood flows. *Microvasc. Res.*, 77, 265–272.
- Ziherl, P. and Svetina, S. (2007). Flat and sigmoidally curved contact zones in vesicle–vesicle adhesion. *Proc. Natl. Acad. Sci. USA*, 104, 761–765.

